Electrically detected-magnetic-resonance identifications of defects at 4H-SiC(000 $\bar{1}$)/SiO$_2$ interfaces with wet oxidation

T. Umeda (iD), Y. Kagoyama, K. Tomita, Y. Abe (iD), M. Sometani (iD), M. Okamoto (iD), S. Harada (iD), and T. Hatakeyama (iD)

View Online   Export Citation   CrossMark

ARTICLES YOU MAY BE INTERESTED IN

Study on the charging current of surface traps in AlGaN/GaN high electron mobility transistors with a slot gate structure
Applied Physics Letters 115, 152105 (2019); https://doi.org/10.1063/1.5111494

Structure and energetics of carbon defects in SiC (0001)/SiO$_2$ systems at realistic temperatures: Defects in SiC, SiO$_2$, and at their interface
Journal of Applied Physics 126, 145302 (2019); https://doi.org/10.1063/1.5100754

Electrically detected magnetic resonance study of barium and nitric oxide treatments of 4H-SiC metal-oxide-semiconductor field-effect transistors
Journal of Applied Physics 126, 145702 (2019); https://doi.org/10.1063/1.5120704

Electrically detected-magnetic-resonance identifications of defects at 4H-SiC(000$\bar{1}$)/SiO$_2$ interfaces with wet oxidation

View Online   Export Citation   CrossMark

T. Umeda,[1,a)] (iD) Y. Kagoyama,[1] K. Tomita,[1] Y. Abe,[1] (iD) M. Sometani,[2] (iD) M. Okamoto,[2] (iD) S. Harada,[2] (iD) and T. Hatakeyama[2] (iD)

AFFILIATIONS

[1]Institute of Applied Physics, University of Tsukuba, Tsukuba 305-8573, Japan
[2]National Institute of Advanced Industrial Science and Technology (AIST), Tsukuba 305-8569, Japan

[a)]Author to whom correspondence should be addressed: umeda@bk.tsukuba.ac.jp

ABSTRACT

We present electrically detected-magnetic-resonance (EDMR) identification of major and minor interface defects at wet-oxidized 4H-SiC(000$\bar{1}$)/SiO$_2$ interfaces for C-face 4H-SiC metal-oxide-semiconductor field-effect transistors. The major interface defects are identified as c-axial types of carbon-antisite-carbon-vacancy ($C_{Si}V_C$) defects. Their positive ($+1$) charge state generates a spin-1/2 EDMR center named "C-face defects" and behaves as an interfacial hole trap. This center is responsible for the effective hydrogen passivation of the C face. We also identify a minor type of interface defect at this interface called "$P8$ centers," which appear as spin-1 centers. Judging from their similarity to the $P7$ centers (divacancies, $V_{Si}V_C$) in SiC, they were assigned to be a sort of basal-type interfacial $V_{Si}V_C$ defect. Since both the $C_{Si}V_C$ and $V_{Si}V_C$ defects are known as promising single photon sources (SPSs) in SiC, the wet oxidation of the C face will have good potential for developing SPSs embedded at SiC surfaces.

Published under license by AIP Publishing. https://doi.org/10.1063/1.5116170

4H-SiC metal-oxide-semiconductor field-effect transistors (MOSFETs) are promising high-power and ultra-low-energy-loss switching transistors for next-generation power electronics. The standard 4H-SiC MOSFETs are fabricated on the front side of 4H-SiC(0001) wafers (the "Si face") in association with the thermal oxidation of the Si face in dry O$_2$ ambience.[1] On the other hand, the back side of the same wafer, i.e., 4H-SiC(000$\bar{1}$) surface or "C face," exhibits quite different behaviors. For the C face, wet oxidation in H$_2$O ambience is extremely useful for fabricating high-quality MOS interfaces.[2,3] For instance, the field-effect mobility (μ_{FE}) easily exceeds 70 cm^2 V^{-1} s^{-1} in wet-oxidized C-face MOSFETs, which is much higher than the standard values ($\leq$40 cm^2 V^{-1} s^{-1}) in Si-face MOSFETs.[4,5] While the reason behind such a drastic improvement is still a mystery, it is commonly held that interface defects associated with the wet oxidation are closely related to this behavior.[6] The wet oxidation is also important for other useful SiC surfaces such as 4H-SiC($\bar{1}$100) ("m face") and 4H-SiC(11$\bar{2}$0) ("a face"), as these surfaces exhibit a similar sensitivity to the wet oxidation.[7] To reveal interface defects related to the wet oxidation, we have so far applied electrically detected magnetic resonance (EDMR) spectroscopy to the wet-oxidized C face and found some characteristic interface defects

there,[6,8] including one major type called "C-face defect." However, their microscopic origins still remain unclear.

In this Letter, we identify the origin of the C-face defects on the basis of their hyperfine (HF) interaction due to a ^{13}C nuclear spin. The resolved ^{13}C HF interaction clearly indicates that the C-face defects belong to the family of positively charged carbon-antisite-carbon-vacancy complexes, $C_{Si}V_C(+)$. This type of defect is known as a fundamental defect in p-type 4H-SiC. In the bulk, four types of bulk $C_{Si}V_C(+)$ have been identified,[9] as summarized in Figs. 1(a) and 1(b). In contrast, the wet oxidation of the C face selectively generates c-axial types of $C_{Si}V_C$ at the interface [Figs. 1(a) and 1(c)], which is believed to correlate with atomistic features of wet oxidation and the C face. Moreover, we here show the presence of other characteristic interface defects at the wet-oxidized C face, labeled "$P8$ centers." They are spin-1 ESR centers belonging to the family of divacancy defects ($V_{Si}V_C$, the $P6/P7$ centers[10]). It is worth noting that both the $C_{Si}V_C$ and $V_{Si}V_C$ defects are known as promising single photon sources (SPSs) in SiC.[11,12] Thus, we can expect that the wet oxidation of the C face has potential for exploring SPSs embedded at SiC surfaces.

For EDMR measurements, n-channel lateral C-face 4H-SiC MOSFETs (gate length/width = 2/200 μm) were prepared using a 4°-off
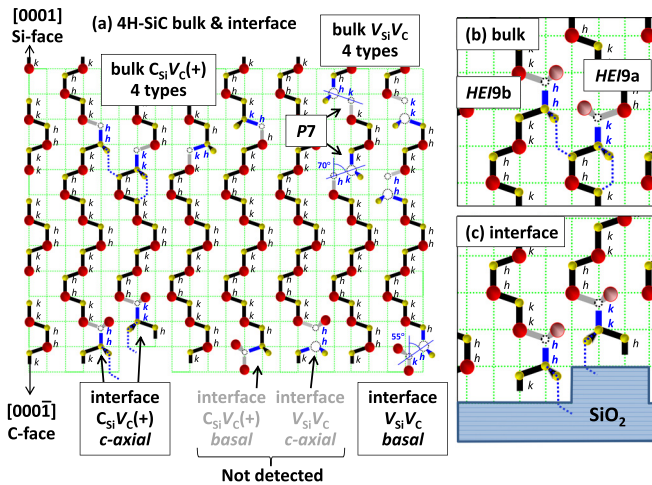
FIG. 1. Atomic models for interface defects at the wet-oxidized 4H-SiC(0001̄)/SiO₂ interface and for bulk $C_{Si}V_C(+)$ centers[9] and bulk $V_{Si}V_C$ centers[10] in 4H-SiC. (a) In the upper part, bulk $C_{Si}V_C$ and $V_{Si}V_C$ defects (hh, kk, hk, and kh types) are displayed. In the lower part, interface defects at the C face are shown. Blue bonds express unpaired-electron orbitals in $C_{Si}V_C$ and $V_{Si}V_C$, which are located on a C_{Si} atom and on three C atoms of the V_{Si} side, respectively. (b) Bulk c-axial $C_{Si}V_C(+)$ centers (HEI9a and HEI9b centers).[9] (c) Interface c-axial $C_{Si}V_C(+)$ centers (indistinguishable hh and kk types). Blue dotted lines represent the periodicity of their 2nd nearest neighbors.

p-epitaxial layer (net acceptor concentration $\approx 5 \times 10^{15}$ cm^{-3}).[6,13] Wet oxidation at 1000 °C (oxide thickness = 60 nm) and H₂ postoxidation anneal (POA) at 1100 °C were applied to the MOSFETs. We have already reported that EDMR observations on the C-face defects were successful only in the wet oxidation of the C face.[6,13] In fact, the C-face defects were not observed in dry-oxidized C-face MOSFETs with the same epitaxial layer, the same implanted source/drain/well regions, and the same thermal history.[8] We also confirmed that H₂ POA after the dry oxidation is not useful to create the C-face defects and the P8 centers. It is also sure that these centers are not implantation damages because they were not observable in SiC-MOSFETs with an implanted (10^{20} cm^{-3}) channel region.[13]

Their EDMR signals increased after γ-ray irradiation due to breaking of the hydrogen (H) passivation of the C-face defects.[6] In this work, we further tried to maximize their EDMR signals by applying moderate postoxidation annealing at 900 °C in N₂ ambience, which remarkably damages the H passivation of C-face MOSFETs.[4] After the 900 °C anneal treatment, the maximum μ_{FE} of the MOSFETs decreased from 80 to 28 cm^2 V^{-1} s^{-1}. We then performed room-temperature EDMR measurements on the annealed C-face MOSFETs by utilizing either the gate-controlled-diode (GCD) EDMR mode or bipolar-amplification-effect (BAE) EDMR mode.[14] We found that the C-face defects were detectable in both the modes, and the GCD EDMR mode gives us a better signal-to-noise ratio for them (instead, the BAE mode gave us larger current changes). In this mode, a forward current of 50–60 nA was driven from the drain/source region to the well region, under applying a gate bias (V_G) of −10 V. The negative V_G was indispensable for increasing the EDMR signals of the C-face defects because they can be converted from ESR-inactive states (neutral states) into ESR-active states (+1 charge states) by

capturing holes.[6] The EDMR signals (current changes induced by ESR transitions) were excited by a microwave of 9.462 GHz and 200 mW and were amplified by a lock-in amplifier synchronized to a magnetic-field modulation at 1.56 kHz.

Figure 2(a) shows a typical EDMR spectrum of the C-face defects in the annealed C-face 4H-SiC MOSFET. The spectrum clearly shows a doublet HF splitting of 1.1 mT, which is a characteristic signature of the C-face defects.[6,8] Figure 2(c) examines angular dependences of the EDMR signals, which can be well fitted by three central solid lines. These lines were simulated by adopting an electron spin (S) of 1/2, a C_{3v} (c-axial) symmetry, the g tensor shown in Table I, and with/without an isotropic doublet HF splitting of 1.1 mT. All the above signatures are consistent with those of the C-face defects.[6]

Looking carefully at both tails of the EDMR signals [Fig. 2(b)], we find a weak doublet HF splitting due to a ^{13}C isotope ($I = 1/2$, natural abundance = 1.1%). Blue solid lines express simulated ^{13}C HF doublets, which were made from two replicas of the experimental spectrum shown in Fig. 1(a). The relative intensity of the replicas was set to be 0.55% in the whole spectrum. By assuming appropriate smooth baselines [dashed blue lines in Fig. 2(b)], the simulated ^{13}C HF doublets can excellently reproduce the tails of the EDMR signals. In Fig. 2(c), we analyzed the angular dependences of the ^{13}C HF splitting (solid symbols). In the ^{13}C HF doublets, we could resolve one side of additional HF doublets (open symbols) due to the 1.1-mT splitting. As shown in the figure, both the ^{13}C HF and 1.1-mT doublets are well simulated by solid lines, which are calculated using a ^{13}C HF tensor shown in Table I.

As shown in Table I, the determined ^{13}C HF tensor is similar to those of the known $C_{Si}V_C(+)$ centers (the HEI9a and HEI9b centers)
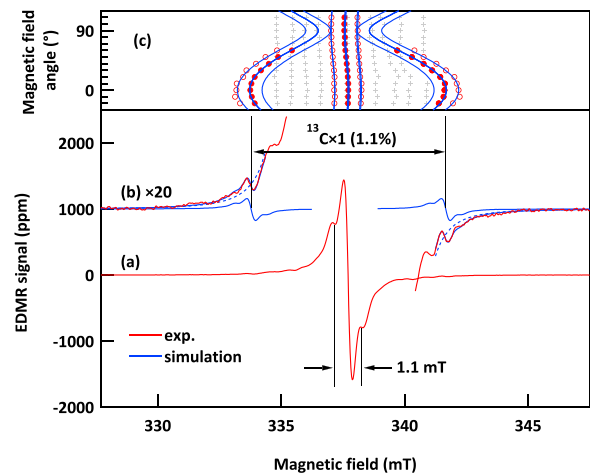

FIG. 2. (a) EDMR spectrum of C-face defects in annealed C-face 4H-SiC MOSFETs with wet oxidation (SiO₂ thickness = 60 nm). The magnetic field (**B**) was modulated by an amplitude of 0.25 mT and the spectrum was measured for **B**//[0001̄]. (b) A doublet ^{13}C HF structure of C-face defects. Blue lines indicate simulation of ^{13}C HF doublets (see details in the text). (c) Angular maps of C-face defects. Solid and open circles represent their resonant fields for without and with an isotropic 1.1-mT HF splitting, respectively. The magnetic field was rotated from −30° to 120° where **B**//[0001] for 0° and **B**//[1̄1̄20] for 90°. Solid lines are simulated by using the g and ^{13}C HF tensors listed in Table I. There are other minor defects which revealed isotropic signals (see grayed symbols). They are assigned to annealing damages because they were absent before annealing.

TABLE I. Spin-Hamiltonian parameters of C-face defects at the 4H-SiC(000$\bar{1}$)/SiO$_2$ interface and bulk C$_{Si}V_C$(+) centers in p-type 4H-SiC. The spin-Hamiltonian in this system is defined as $H = \mu_B \mathbf{S} \cdot \mathbf{g} \cdot \mathbf{B} + \mathbf{S} \cdot \mathbf{A} \cdot \mathbf{I} - g_n \mu_n \mathbf{I} \cdot \mathbf{B}$,[15] where μ_B is the Bohr magneton, $\mathbf{S}$ is an electron spin operator, $\mathbf{g}$ is a gyromagnetic-factor tensor, $\mathbf{B}$ is an external magnetic-field vector, $\mathbf{A}$ is a ^{13}C HF tensor, and the third term represents a nuclear-spin Zeeman energy for a ^{13}C nucleus. Both the $\mathbf{g}$ and $\mathbf{A}$ tensors are well described by axially symmetric tensors (e.g., $A_{zz} \equiv A_{||}$ and $A_{xx} = A_{yy} \equiv A_{\perp}$) with respect to the c axis.

Center	Origin (charge)	Spin (symmetry)	g		A(^{13}C) (mT)	
			$g_{//}$	$g_{\perp}$	$A_{//}$	$A_{\perp}$
Wet-oxidized C-face 4H-SiC MOSFETs, present and Ref. 6						
C-face	Interfacial	1/2	2.0018	2.0027	8.0	2.1
defect	C$_{Si}V_C$(+)	(C$_{3v}$)				
p-type 4H-SiC bulk, Ref. 9						
HEI9a	C$_{Si}V_C$(+) kk site	1/2	2.00227	2.00408	8.25	2.27
HEI9b	C$_{Si}V_C$(+) hh site	(C$_{3v}$)	2.00195	2.00379	9.95	3.71

in p-type 4H-SiC;[9] specifically, we found good agreement between the present center and the HEI9a center. In these bulk C$_{Si}V_C$(+), a main ^{13}C HF interaction is generated from a C$_{Si}$ atom of C$_{Si}V_C$ where an electron spin is localized on a strongly p-like orbital [blue bonds in Figs. 1(a) and 1(b)]. Moreover, comparing the C-face defects with the HEI9a/b centers, their electron spin (1/2), their symmetry (C$_{3v}$), and their charge state (+1) are also consistent with each other. Therefore, we conclude that the C-face defects belong to the family of HEI9a/b centers, i.e., they are c-axial types of interface C$_{Si}V_C$(+) centers at the wet-oxidized C face, as illustrated in Figs. 1(a) and 1(c).

However, a few fundamental questions on the above model remain. The first is an apparent inconsistency in the g tensors between the C-face defects and the HEI9a/b centers (Table I). We attribute this inconsistency to a perturbation of the interface. In fact, we already reported such a perturbation on the g tensor for the cases of typical dopants (nitrogen donors[16] and phosphorous donors[17]) when they are incorporated into the close vicinity of the interface.

The second is why only one type of EDMR center was observable at the interface despite four types of ESR centers distinguishable in bulk 4H-SiC [Fig. 1(a)]. In the bulk, two c-axial types [kk and hh types, see Fig. 1(b)] are distinguishable as the HEI9a and HEI9b centers, respectively.[9] A distinguishable point between them is the periodicity of their 2nd nearest neighbors (NNs), which are indicated by the blue dotted lines in Fig. 1(b). For the HEI9a and HEI9b centers, each 2nd NN atom connects to either the same column or a next column, respectively. Such a difference results in the distinguishable ESR centers. In contrast, at the interface shown in Fig. 1(c), each 2nd NN atom should connect to the amorphous SiO$_2$ network. This constraint supposedly makes the hh and kk types indistinguishable at the interface.

The interface C$_{Si}V_C$ defects reasonably account for the effective H passivation of the C face.[2–4] Our previous ESR study confirmed that the HEI9/10 centers (C$_{Si}V_C$) are one of the most reactive ESR centers to the H passivation in p-type 4H-SiC.[18] An unpaired electron on the C$_{Si}$ atom can be passivated in the form of C-H bonds, and such passivation can be removed at above 800 °C.[18] This temperature range is consistent with the degradation temperature observed for wet-oxidized C-face MOSFETs.[4]

In addition to the C$_{Si}V_C$ defects, there is a minor but interesting ESR center at the wet-oxidized C face, which we call the P8 centers. Figure 3(a) shows EDMR signals of two P8 centers (P8a and P8b) that

were only detectable in wet-oxidized C-face MOSFETs. These P8 centers exhibit a large zero-field splitting (fine splitting) due to a close pair of two electron spins ($S = 1$). From the angular-map analyses shown in Fig. 3(b), their fine-splitting constants (D and E[10]) are estimated to be $D = 50$ mT and $D = 43$ mT for P8a and P8b, respectively, and $E \leq 1$ mT for both the centers. These parameters are quite similar to
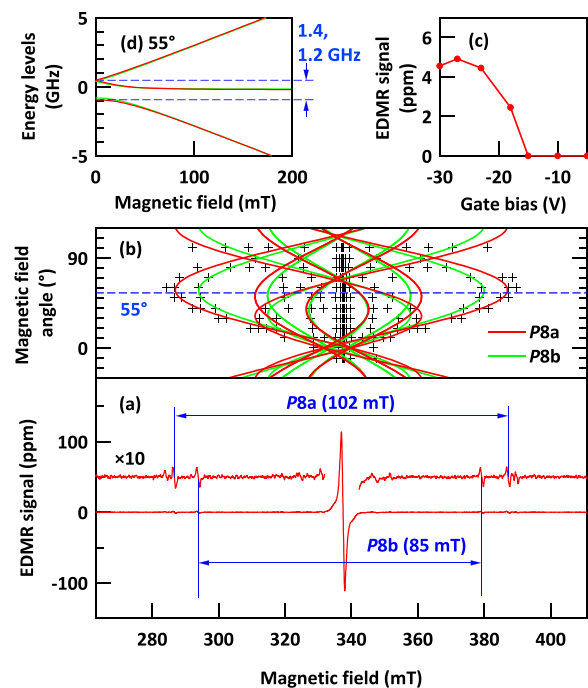

FIG. 3. (a) EDMR spectrum of P8 centers at the wet-oxidized 4H-SiC(000$\bar{1}$)/SiO$_2$ interface. This spectrum was measured for a forward current of 85 nA under $V_G = -27$ V in wet-oxidized (nonannealed) C-face MOSFETs. A strong central line arises from C-face defects (see Fig. 2). At least two spin-1 ESR centers (P8a and P8b) are resolved in the figure. (b) Angular maps of P8 centers. Magnetic-field rotation was set to be the same manner as used in Fig. 2. Solid lines are simulated angular patterns (see the text). (c) Gate-bias dependence of P8 centers. (d) Energy-level calculations on spin-1 systems of P8a and P8b (red and green lines, respectively) for a magnetic-field angle of 55°.

those of the $P7$ centers in bulk 4H-SiC ($D = 43$–48 mT and $E < 0.7$ mT).[10,19] The $P7$ centers are basal-type divacancies ($V_{Si}V_C$) configured by 70°-off from the c direction, as is drawn on the right-hand side of Fig. 1(a). Judging from the similarity between the $P8$ and $P7$ centers, we assign the $P8$ centers to be a sort of interfacial $V_{Si}V_C$ defect in a basal configuration. The $P8$ centers became detectable under a strong negative gate bias [Fig. 3(c)]. This is due to the gate-bias control of $P8$'s charge state, similar to the case of the C-face defects.[6] One notable difference between the $P8$ and $P7$ centers is seen in their symmetrical axes where each fine splitting has a maximum. For the $P8$ center, the symmetrical axis is tilted by about 55° from the c axis [Fig. 3(b)], which is deviated from 70° for the $P7$ centers[10] [see Fig. 1(a)]. The tilt angle of 55° implies that the $P8$ centers are slightly rotated from the original $V_{Si}V_C$ centers, like shown in the right-hand bottom side of Fig. 1(a), possibly due to an influence of the interface.

Looking over the above results, one finds an interesting contrast: basal types of $C_{Si}V_C$ (kh and hk types) are missing, while c-axial types of $V_{Si}V_C$ (kk and hh types) are absent at the interface [see the bottom of Fig. 1(a)]. Unfortunately, we do not have a clear answer to this question; however, we believe that this is strongly correlated with the wet-oxidation mechanism of the C face. Some tentative reasons are given with the help of Fig. 1(a). As seen in the figure, the basal types of interface $C_{Si}V_C$ place V_C as well as surrounding Si atoms in the interface side, while the c-axial types place them in the bulk side. As a result, the basal types are expectedly much more reactive to O atoms than the c-axial types, which may promote the selective annihilation of the basal types. With the same analogy, we reasonably expect that the amount of $P8$ centers (the basal-types $V_{Si}V_C$) should be much less than that of C-face defects (the c-axial types of $C_{Si}V_C$). On the other hand, "missing" c-axial types of $V_{Si}V_C$ [bottom of Fig. 1(a)] possess unpaired-electron orbitals in the interface side, which are directly exposed to the oxidants. As a result, the c-axial types of interface $V_{Si}V_C$ may be difficult to survive.

Another interesting feature is that both interface defects are "vacancy types." Also for the Si face, the formation of interfacial Si vacancies (V_{Si}) was reported via EDMR analyses.[20] It is worth mentioning that the bistability of $C_{Si}V_C$ and V_{Si} exists in SiC.[9,21] In p-type 4H-SiC (note that the present channel region is p-type), $C_{Si}V_C$ should be more stable than V_{Si}. We imagine that the oxidation of the C face may initiate the extraction of a Si atom from SiC, forming a V_{Si}-like structure because the oxidation requires a reaction between Si and O. Such a precursor may be subsequently stabilized into a $C_{Si}V_C$ form. The details of such atomistic mechanisms will be revealed by theoretical calculations in the future. Here, we should emphasize that the formation of $C_{Si}V_C$ and $V_{Si}V_C$ can only be successful in cooperation with H atoms. When the C face is oxidized by dry O_2, its interface generates sp^2-bonded C cluster defects,[8] instead of the $C_{Si}V_C$ and $V_{Si}V_C$ defects. We observed the isotropic HF splitting of 1.1 mT for $C_{Si}V_C$, suggesting the presence of a ^{1}H HF interaction.[6] Such a H atom possibly attaches to the V_C side of $C_{Si}V_C$. Since this HF interaction was alive even after the 900 °C anneal treatment, the survival of a Si-H bond in the V_C side may occur. Another possible assignment for the 1.1-mT HF splitting may be ^{29}Si HF interactions of three Si atoms of V_C. Both the models will be inspected in the future.

The identification of interface defects in this study rehighlights the importance of wet oxidation of the C-face, as both $C_{Si}V_C$ and $V_{Si}V_C$ are known as promising SPSs in SiC.[11,12] In fact, the first step in creating SPSs in SiC-MOSFETs has been recently achieved using wet-oxidized C-face MOSFETs.[22,23] In Fig. 3(d), we found zero-field splittings of 1.40 GHz and 1.21 GHz for the $P8$a and $P8$b centers. Note that the $P8$ centers may be more suitable to SPSs rather than bulk $V_{Si}V_C$, because the $P8$ centers are easily observable at room temperature.

In summary, we have clarified the microscopic origins of major and minor interface defects at wet-oxidized 4H-SiC(000$\bar{1}$)/SiO$_2$ interfaces in C-face 4H-SiC MOSFETs. The major defects, called C-face defects,[6,8] have been identified as c-axial types of interface $C_{Si}V_C$ defects. We also found a minor type of interface defect (the $P8$ centers), exhibiting spin-1 ESR centers with a zero-field splitting of 1.2–1.4 GHz. They were ascribed to a sort of basal-type interfacial $V_{Si}V_C$ defects. The selective formation of c-axial $C_{Si}V_C$ and basal $V_{Si}V_C$ at the interface is believed to strongly correlate with atomistic mechanisms of wet oxidation of the C-face, which were briefly discussed in conjunction with the interface structure.

REFERENCES

[1]T. Kimoto and J. A. Cooper, *Fundamentals of Silicon Carbide Technology* (Wiley, Singapore, 2014).

[2]K. Fukuda, M. Kato, K. Kojima, and J. Senzaki, Appl. Phys. Lett. **84**, 2088 (2004).

[3]K. Kita, H. Hirai, H. Kajifusa, K. Kuroyama, and K. Ishinoda, Microelectron. Eng. **178**, 186 (2017).

[4]S. Harada, M. Kato, T. Yatsuo, K. Fukuda, and K. Arai, Mater. Sci. Forum **600-603**, 675 (2009).

[5]T. Hatakeyama, T. Masuda, M. Sometani, S. Harada, D. Okamoto, H. Yano, Y. Yonezawa, and H. Okumura, Appl. Phys. Express **12**, 021003 (2019).

[6]T. Umeda, M. Okamoto, H. Yoshioka, G.-W. Kim, S. Ma, R. Arai, T. Makino, T. Ohshima, and S. Harada, ECS Trans. **80**, 147 (2017).

[7]T. Endo, E. Okuno, T. Sakakibara, and S. Onda, Mater. Sci. Forum **600-603**, 691 (2009).

[8]Y. Kagoyama, M. Okamoto, T. Yamasaki, N. Tajima, J. Nara, T. Ohno, H. Yano, S. Harada, and T. Umeda, J. Appl. Phys. **125**, 065302 (2019).

[9]T. Umeda, J. Isoya, T. Ohshima, N. Morishita, H. Itoh, and A. Gali, Phys. Rev. B **75**, 245202 (2007).

[10]N. T. Son, P. Carlsson, J. ul Hassan, E. Janzén, T. Umeda, J. Isoya, A. Gali, M. Bockstedte, N. Morishita, T. Ohshima, and H. Itoh, Phys. Rev. Lett. **96**, 055501 (2006).

[11]S. Castelletto, B. C. Johnson, V. Ivády, N. Stavrias, T. Umeda, A. Gali, and T. Ohshima, Nat. Mater. **13**, 151 (2014).

[12]W. F. Koehl, B. B. Buckley, F. J. Heremans, G. Calusine, and D. D. Awschalom, Nature **479**, 84 (2011).

[13]T. Umeda, M. Okamoto, R. Kosugi, R. Arai, Y. Sato, S. Harada, T. Makino, and T. Ohshima, ECS Trans. **58**, 55 (2013).

[14]T. Aichinger and P. M. Lenahan, Appl. Phys. Lett. **101**, 083504 (2012).

[15]J. Isoya, T. Umeda, N. Mizuochi, N. T. Son, E. Janzén, and T. Ohshima, Phys. Status Solidi B **245**, 1298 (2008).

[16]T. Umeda, K. Esaki, R. Kosugi, K. Fukuda, T. Ohshima, N. Morishita, and J. Isoya, Appl. Phys. Lett. **99**, 142105 (2011).

[17]T. Umeda, G.-W. Kim, T. Okuda, M. Sometani, T. Kimoto, and S. Harada, Appl. Phys. Lett. **113**, 061605 (2018).

[18]K. Murakami, S. Tanai, T. Okuda, J. Suda, T. Kimoto, and T. Umeda, Mater. Sci. Forum **858**, 318 (2016).

[19]The D and E parameters of $P8$ are also close to those of the $V_{Si}N_C$ centers (divacancy + N atom) reported in H. J. von Bardeleben, J. L. Cantin, A. Csóré, A. Gali, E. Rauls, and U. Gerstmann, Phys. Rev. B **94**, 121202(R) (2016). However, since the $P8$ centers were absent in N-doped implanted channel[13] and basal types of $V_{Si}N_C$ centers have not been found so far, we assigned $P8$ to a family of basal-type divacancies.

[20]C. J. Cochrane, P. M. Lenahan, and A. J. Lelis, J. Appl. Phys. **109**, 014506 (2011).

[21]T. Umeda, N. T. Son, J. Isoya, E. Janzén, T. Ohshima, N. Morishita, H. Itoh, A. Gali, and M. Bockstedte, Phys. Rev. Lett. **96**, 145501 (2006).

[22]Y. Abe, T. Umeda, M. Okamoto, R. Kosugi, S. Harada, M. Haruyama, W. Kada, O. Hanaizumi, S. Onoda, and T. Ohshima, Appl. Phys. Lett. **112**, 031105 (2018).

[23]Y. Abe, T. Umeda, M. Okamoto, S. Onoda, M. Haruyama, W. Kada, O. Hanaizumi, R. Kosugi, S. Harada, and T. Ohshima, Mater. Sci. Forum **924**, 281 (2018).